Journal of Catalysis **190,** 309–319 (2000)
doi:10.1006/jcat.2000.2768, available online at http://www.idealibrary.com on IDEAL®

Activity, Selectivity, and Sulfur Resistance of Pt/WO_x–ZrO_2 and Pt/Beta Catalysts for the Simultaneous Hydroisomerization of *n*-Heptane and Hydrogenation of Benzene

M. A. Arribas, F. Márquez, and A. Martínez[1]

Instituto de Tecnología Química, Avenida de los Naranjos s/n, 46022 Valencia, Spain

Received July 22, 1999; revised November 19, 1999; accepted November 19, 1999

Bifunctional Pt/WO_x–ZrO_2 (Pt/WZr, 12.7 wt% W) and Pt/Beta (Si/Al = 12) catalysts have been studied for the simultaneous *n*-alkane hydroisomerization and aromatic hydrogenation using a *n*-heptane/benzene feed mixture (25 wt% benzene) at 3.0 MPa and temperatures in the 473–573 K range. The catalysts were characterized by X-ray diffraction, adsorption–desorption of N_2, laser Raman spectroscopy (for WZr), temperature-programmed desorption (TPD) of NH_3, CO chemisorption, temperature-programmed reduction (TPR), and X-ray photoelectron spectroscopy (XPS). In the absence of sulfur, the Pt/WZr catalyst was more active than Pt/Beta, indicating that the former has some acid sites of a higher acid strength, as suggested also by NH_3–TPD. At constant *n*-C_7 conversion, the selectivity to *iso*-C_7 was similar for both catalysts (ca. 87% for Pt/Beta and 90% for Pt/WZr at 75% conversion), but the concentration of high octane di + tribranched C_7 isomers was slightly higher for Pt/WZr. Under the reaction conditions used, benzene was totally hydrogenated on both catalysts, with a selectivity to cyclohexane (CH) + methylcyclopentane (MCP) above 90%. The MCP/CH ratio was higher for Pt/Beta. In the presence of 200 ppm sulfur, the Pt/Beta catalyst retained a much higher isomerization activity than Pt/WZr. Furthermore, the conversion of benzene was kept at 100% for the zeolite-based catalyst in the range of TOS studied, while it decreased from 100% to ca. 0 and 4% after ca. 300 min on stream for Pt/WZr samples containing 0.6 and 1% Pt, respectively. The lower sulfur resistance of Pt/WZr could be explained by a too strong interaction of part of the Pt with surface W^{6+} species in the WO_x–ZrO_2 support, as evidenced by TPR and XPS measurements, although the possibility of a different deactivation mechanism for both Pt/Beta and Pt/WZr catalysts and/or the formation of sulfur-resistant electron-deficient Pt species in the zeolite cavities cannot be discarded. Deactivation of the hydrogenation sites in the presence of sulfur was a reversible process for the two catalysts, while the loss of isomerization activity was seen to be almost reversible for Pt/Beta and irreversible for Pt/WZr.

Key Words: ***n*-heptane isomerization; benzene hydrogenation; Pt catalysts; tungsten–zirconia; zeolite Beta; sulfur poisoning.**

1. INTRODUCTION

Environmental concerns have prompted legislation to limit the amount of total aromatics, and particularly of benzene, in gasoline. Reduction of aromatics will have a negative impact on gasoline octane that has to be compensated by other means. An interesting alternative would be to increase the contribution of high-octane branched paraffins in the gasoline pool through the hydroisomerization of the corresponding normal paraffins. At present, isomerization of light naphtha components (*n*-C_5/*n*-C_6) is successfully carried out in the presence of hydrogen and a bifunctional catalyst, typically formed by Pt supported on an acidic carrier, such as halogen-treated alumina or zeolite of the Mordenite type. While the former catalyst is used at lower reaction temperatures, thus affording higher yields of branched paraffins, it presents the disadvantage of being highly corrosive and highly sensitive to feed impurities, such as water and sulfur (1, 2). On the other hand, it would be desirable to extend the isomerization reaction to normal paraffins larger than C_6. In this case, high isomerization yields, especially of higher octane multibranched components, with minimum losses by hydrogenolysis and hydrocracking, has to be achieved.

In order to eliminate benzene in gasoline while minimizing the octane loss it has been proposed to carry out, in a single step, the saturation of benzene and the hydroisomerization of C_5–C_7 normal paraffins (3). However, this cannot be achieved with the actual bifunctional catalysts used for light naphtha isomerization, for which the concentration of benzene and C_{7+} paraffins in the naphtha feed has to limited in order to preserve their isomerization efficiency. In this respect, it has been shown that the addition of even low amounts of benzene to the feed causes a suppression of the isomerization activity of the Pt/mordenite catalysts (4–6), while the presence of C_{7+} *n*-paraffins leads to excessive gas yields by hydrocracking of the highly branched isomers (7). In the case of Pt/mordenite, the reduction of the isomerization activity by aromatics has been explained by a competition for adsorption on the zeolite acid sites of the

[1] To whom correspondence should be addressed. Fax: +34-96 387 78 09. E-mail: amart@itq.upv.es.

0021-9517/00 $35.00

aromatic and the olefinic intermediates of the isomerization reaction and by diffusion limitations caused by the adsorbed aromatic species (4, 8). Therefore, it would be interesting to design alternative catalysts capable of carrying out simultaneously the hydrogenation of benzene and the hydroisomerization of C_{7+} normal paraffins with high selectivity to high-octane branched isomers.

Bifunctional catalysts prepared by supporting a noble metal (Pt, Pd) on zeolite Beta (7, 9–12) and tungsten-promoted zirconium oxide (13–17) have been shown to display high selectivity for the hydroisomerization of C_6–C_7 normal paraffins at moderate pressures in the presence of hydrogen. However, for both types of catalysts the influence of the presence of aromatics, and particularly benzene, on the isomerization activity and selectivity has not been studied yet. Furthermore, the resistance of the catalyst toward sulfur poisoning is an important aspect of the hydroisomerization and hydrogenation processes. However, despite the resistance to sulfur poisoning of Pt(Pd)–zeolite catalysts is well documented for both the hydroisomerization (18, 19) and hydrogenation (20–23) reactions, there are no studies concerning the influence of sulfur on the catalytic performance of Pt/WO_x–ZrO_2 catalysts during the hydroisomerization reaction.

In this work we have studied the hydroisomerization of *n*-heptane in the presence of large amounts (25 wt%) of benzene over two bifunctional catalysts, Pt/WO_x–ZrO_2 and Pt/Beta. The catalytic performance of these two materials in the presence of sulfur has also been evaluated by adding 200 ppm S to the *n*-C_7/benzene feed mixture. As will be shown here, while in the absence of sulfur both type of catalysts were suitable for carrying out the simultaneous isomerization of *n*-C_7 and hydrogenation of benzene, the sulfur resistance strongly depended on the nature of the support, being significantly higher for the zeolite-based catalyst.

2. EXPERIMENTAL

2.1. Preparation of Catalysts

WO_x–ZrO_2 was prepared similarly to the procedure described in (24, 25) as follows: first $Zr(OH)_4$ was obtained by hydrolysis of $ZrOCl\,8H_2O$ (Riedel-de Haën) with an aqueous solution of NH_4OH (25 wt%, Merck) until a pH of approximately 9.6 was reached. The precipitate was filtered, washed with distilled water, and dried at 433 K overnight. Then, $Zr(OH)_4$ was added to an aqueous solution of ammonium metatungstate [$(NH_4)_6\,H_2W_{12}O_{40}\,nH_2O$, Fluka] in a liquid/solid ratio of 3 cm^3/g and agitated at room temperature for 1 h, followed by evaporation of water in a rotary evaporator and drying at 433 K for 12 h. After that, the solid was calcined in flowing dry air (120 cm^3/min for 3 g of sample) at 1073 K for 3 h at a heating rate of 2 K/min. The material obtained contained 12.7 wt% tungsten as determined by ICP. The calcined WO_x–ZrO_2 was finally impregnated with a solution of chloroplatinic acid in 0.2 N HCl to obtain a nominal concentration of Pt of 0.6 wt% (sample 0.6Pt/WZr) and 1 wt% (sample 1Pt/WZr) and calcined again at 773 K for 3 h.

The HBeta zeolite (acid form) was obtained from PQ Corp (Si/Al = 12) and was used without further treatments. The zeolite was then impregnated with 1 wt% Pt as described above and finally calcined at 773 K for 3 h.

The Pt/WO_x–ZrO_2 and Pt/Beta samples were finally reduced *in situ* in a flow of H_2 (300 cm^3/min for 3 g of catalyst) for 2 h at 523 and 723 K, respectively. It has been reported (26, 27) that in the case of Pt/WO_x–ZrO_2 high reduction temperatures (above 673 K) have to be avoided in order to prevent extensive reduction of W^{6+} species that would modify the nature of the tungsten–zirconia support. In fact, a better isomerization activity is usually obtained when reduction temperatures in the range of 523–623 K are applied to the Pt-promoted tungsten–zirconia catalysts (27).

2.2. Catalyst Characterization

Powder X-ray diffraction (XRD) was performed in a Philips PW 1830 apparatus using CuK_α radiation. The crystallinity of the Beta zeolite was calculated from the intensity of the 22° 2θ peak in reference to a standard Beta sample. The percentage of tetragonal zirconia (X_t) present in the tungsten–zirconia samples was estimated from the intensities of the (111) and (11-1) reflections of the tetragonal and monoclinic phase, respectively, and using the equation given in Ref. (28):

$$X_t\,(\%) = \frac{I(111)_t}{I(111)_t + 1.6\,I(11-1)_m}100.$$

Textural properties were determined by N_2 adsorption at 77 K on a ASAP-2000 (Micromeritics) apparatus after pretreating the samples at 673 K and vacuum overnight.

The acidity of the zeolite and WO_x–ZrO_2 supports was determined by temperature programmed desorption (TPD) of NH_3 in a TPD/TPR 2900 equipment (Micromeritics) coupled with a quadrupole mass spectrometer (ThermoStar from Balzers Instruments). Before adsorption of ammonia, about 0.100 g of sample were pretreated at 723 K in oxygen for 1 h and then in argon for 0.5 h and finally in helium for 0.5 h at the same temperature. Then, ammonia was adsorbed at 373 K until saturation and desorbed from 373 K up to 1073 K at a heating rate of 10 K/min while the composition of the desorbed gases was monitored in the mass spectrometer.

Laser-Raman spectroscopy (LRS) was performed on WO_x–ZrO_2 and Pt/WO_x–ZrO_2 in a FT Raman II spectrometer from Bio-Rad, using the 1.064-nm line of a Nd : YAG laser for excitation. The Raman spectra were corrected

for instrumental response using a white light reference spectrum.

Temperature-programmed reduction (TPR) of the Pt catalysts and WZr support was performed in a TPD/TPR Autochem 2910 equipment (Micromeritics) using a TCD. Before the measurements the sample (about 0.1 g) was placed in a quartz cell and pretreated in O_2 flow (30 cm^3/min) at 773 K for 1 h. Then, the sample was heated from room temperature up to 1173 K at a heating rate of 10 K/min while flowing a mixture of 15 vol% H_2 in He through the sample. The amount of H_2 consumed was determined using CuO as a reference sample.

The dispersion of Pt on the zeolite and WZr supports was estimated from the CO adsorption isotherms at 308 K in a ASAP 2010C equipment. Before starting the adsorption, the samples (ca. 0.5 g) were pretreated in He at 623 K and vacuum for 30 min and then reduced in H_2 for 2 h at 523 K for Pt/WZr and 723 K for Pt/Beta. The stoichiometry of CO to Pt was assumed to be unity.

The state of Pt in the calcined and reduced catalysts was determined by X-ray photoelectron spectroscopy (XPS). The X-ray photoelectron spectra were acquired with a surface analysis system (Escalab-210, VG-Scientific) by using the MgK_α (1253.6 eV) radiation of a twin anode in the constant analyser energy mode, with a pass energy of 50 eV. During the spectral acquisition the pressure of the analysis chamber was maintained at 7×10^{-10} mbar. All samples are insulators with a very small amount of carbonaceous impurity on their surfaces. The charging effect was corrected by setting the Cls transition at 284.6 eV. The reproducibility of the peak position was ±0.1 eV. *In situ* reduction experiments were conducted in a high-pressure gas cell (HPGC) mounted directly to the preparation chamber of the spectrometer, so the catalysts could be moved to the analysis chamber without exposure to air. To facilitate the analysis of the samples we obtained self-supporting wafers of 9 mm diameter and ca. 9 mg weight that were fixed on a circular sample holder.

The surface composition was estimated from the corresponding XPS peak area ratios by using the relation

$$\left[\frac{X}{Y}\right]_S = \frac{A_X}{A_Y}\frac{\sigma_Y}{\sigma_X}\frac{\lambda_Y}{\lambda_X}\sqrt{\frac{E_K(X)}{E_K(Y)}},$$

where A, σ, λ, and E_K are the integral of each peak after S-shaped background substraction, the effective ionization cross section, the escape depth, and the photoelectron kinetic energy respectively. Cross section values were taken from Scofield (29) and escape depths were calculated from the formulas given by Vulli and Starke (30). In the case of Pt/Beta sample, and owing to the overlapping of the Al2*p* and Pt4*f* peaks, the concentration of Pt on the zeolite surface was determined using the Pt4*d* transition.

2.3. Catalytic Experiments

The conversion of a *n*-heptane/benzene feed mixture containing 25 wt% benzene was carried out in a self-made down-flow fixed-bed stainless-steel reactor containing a back-pressure regulator (Badger Meter Optipac, Model 945) to keep the system pressure to the desired value. Before being loaded to the reactor, 3 g of catalyst was crushed and sieved to a particle size of 0.25–0.42 mm diameter and diluted with CSi (0.59–0.84 mm particle size) to a constant bed volume of 10 cm^3. Then, the catalyst was reduced *in situ* by gradually increasing the temperature to the desired value (523 and 723 K for Pt/WO_x–ZrO_2 and Pt/Beta samples, respectively) in flowing hydrogen (300 cm^3/min) and kept for 2 h at the given temperature.

The catalytic tests were performed at 3.0 MPa total pressure, H_2/hydrocarbon molar ratio of 10, space velocity (WHSV) of 3.1 h^{-1}, and temperature in the 473–573 K range. For the sulfur resistance experiments, 200 ppm S was added as 2-methylthiophene (2MT) to the *n*-C_7/benzene mixture. The reactor effluent was depressurized, vaporized at 453 K, and analyzed on line at regular intervals in a gas chromatograph (Varian 3800) equipped with a capillary column (Petrocol DH50.2, 50 m × 0.2 mm) and a FID. Complete separation of reactants and products was achieved using the following temperature program in the GC oven: $T_{in} = 313$ K, $t_{in} = 5$ min, rate = 5 K/min, $T_{fin} = 373$ K. Identification of reaction products was done by mass spectrometry and by comparing the retention times with those of available standards.

3. RESULTS AND DISCUSSION

3.1. Catalyst Characterization

The physicochemical characteristics of the WO_x–ZrO_2 and zeolite Beta supports and that of the final Pt-containing catalysts are listed in Table 1.

The WO_x–ZrO_2 sample calcined at 1073 K presents a surface area of 61 m^2/g and the tetragonal ZrO_2 was the predominant crystalline phase present (88%), in agreement with previous data reported for samples prepared in a similar way and having similar tungsten loading (13). A small amount of tetragonal WO_3 crystallites ($2\theta = 23.2°$, 23.7°, and 24.4°) was also observed in the XRD of the WO_x–ZrO_2 and Pt-supported samples (not shown). As observed in Table 1, both the BET surface area and the proportion of tetragonal zirconia in Pt/WZr were little affected by the impregnation of Pt.

The nature of the surface species in the calcined WO_x–ZrO_2 and Pt/WO_x–ZrO_2 samples was also studied by laser-Raman spectroscopy. The features of the Raman spectra (not shown) coincided with those reported for hydrated WO_x–ZrO_2 samples with similar W loading and calcined at similar temperatures (25, 31). Thus, besides the bands at

TABLE 1

Physicochemical Properties of the WO_x–ZrO_2 and Beta Zeolite Supports and Pt-Containing Catalysts

Sample	XRD		Textural properties			NH_3 uptake (cm^3 NTP/g)	Pt dispersion[a] (%)
	% Crystal.	% of ZrO_2 tet.	Area BET (m^2/g)	Total pore volume (cm^3/g)	Micropore volume (cm^3/g)		
WZr	—	90	61	0.10	0.0	3.5	—
0.6Pt/WZr	—	86	63	0.11	0.0	—	47.9
1Pt/WZr	—	88	59	0.11	—	—	20.5
Beta	79	—	579	0.65	0.17	26.0	—
1Pt/Beta	78	—	567	0.68	0.17	—	42.4

[a] From CO chemisorption measurements.

970–997 cm^{-1} assigned to the W=O stretching vibrations of a two-dimensional tungsten oxide species, bands appearing at ca 806, 716, and 274 cm^{-1} were observed, indicating the presence of crystalline WO_3, in agreement with the XRD data.

The acid properties of the WO_x–ZrO_2 and Beta zeolite supports were studied by temperature-programmed desorption (TPD) of NH_3. The results of NH_3 uptake at 373 K (Table 1) indicate that the total amount of acid sites is significantly higher for the zeolite sample. Moreover, the desorption profiles of the two solid acids are presented in Fig. 1. The Beta zeolite shows two main desorption features centered at about 478 and 628 K, which correspond to the desorption of NH_3 interacting with weak and medium-strong acid sites. A weaker and broader peak is also observed at ca. 868 K originated from the desorption of water formed upon dehydroxylation of the zeolite surface, as monitored by GC-MS. On the other hand, the TPD of WO_x–ZrO_2 calcined at 1073 K shows a broad desorption feature in the 423–823 K range. This indicates a wide range of acid strength distribution in the WZr support. The fact that some NH_3 desorbs at temperatures higher than in the zeolite (above 800 K) might suggest that WZr probably contains some acid sites of a higher acid strength than those present in the zeolite. Microcalorimetry results of ammonia adsorption in WO_x–ZrO_2 also revealed the presence of strong acid sites with initial adsorption heats of 150–160 kJ/mol (31).

The TPR profiles of the calcined WO_x–ZrO_2, with and without platinum, and that of the Pt/Beta catalyst are presented in Fig. 2. In the absence of Pt, the WZr shows a broad reduction feature starting at temperatures above 823 K, with two maxima at ca. 873 and 1017 K, which have been ascribed to the partial reduction of W^{6+} species (32). After incorporation of Pt (1 wt%) a low-temperature peak centered at about 360 K is observed, which can be due to the reduction of Pt^{4+} to Pt^{2+}, as suggested in (32). The increase of intensity of the peak at ca. 873 K upon Pt incorporation is probably due to a further reduction of W^{6+} species facilitated by the presence of Pt and evidences a strong interaction between some Pt particles and the WZr support. It has also been suggested that part of the Pt, probably those particles directly interacting with the surface W species, are also reduced at this high temperature (32). The TPR of the Pt/Beta cataslyst presents two reduction features at ca. 405

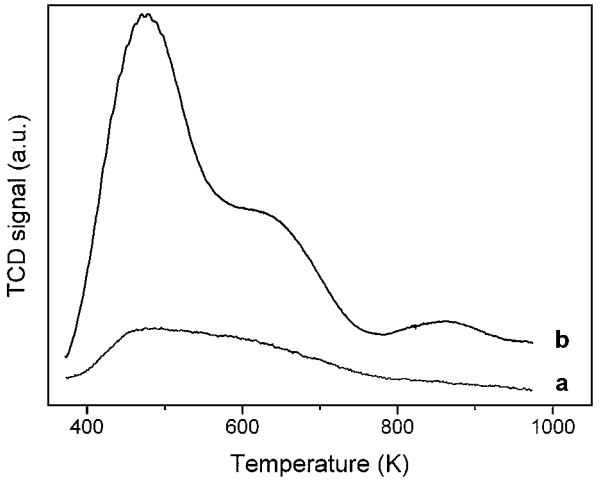

FIG. 1. NH_3–TPD curves of (a) WZr and (b) zeolite Beta.

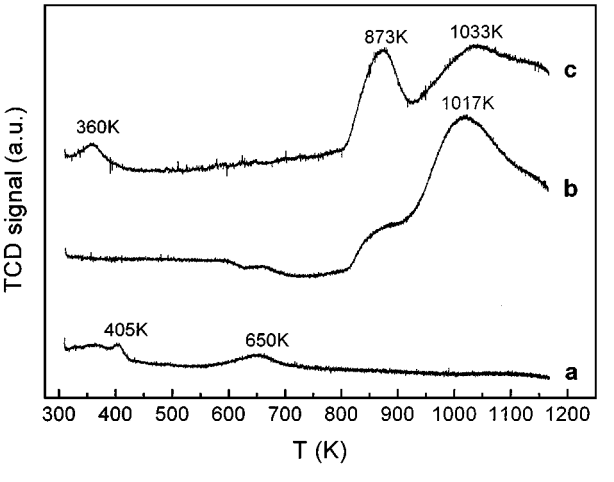

FIG. 2. TPR profiles of (a) 1Pt/Beta, (b) WZr, and (c) 1Pt/WZr samples.

TABLE 2

Binding Energies (eV) of Pt4$f_{7/2}$, W4$f_{7/2}$, Zr3$d_{5/2}$ Transitions for the Calcined and Reduced Pt/Beta and Pt/WO_x–ZrO_2 Catalysts

Sample	Pt4$f_{7/2}$	W4$f_{7/2}$	Zr3$d_{5/2}$	Pt surface composition (wt%)
1Pt/Beta (calcined)	72.1	—	—	0.4
1Pt/Beta (reduced in H_2 at 723 K)	70.4	—	—	0.6
1Pt/WZr	74.9	35.6	182.6	
(calcined)	73.6			1.0
1Pt/WZr	74.0	35.7	182.6	
(reduced in H_2 at 523 K)	71.0	34.6		1.1

and 650 K, which can be assigned to the reduction of Pt^{4+} to Pt^{2+} and of Pt^{2+} to Pt^0, respectively.

The dispersion of Pt in the Pt/WZr (0.6 and 1 wt% Pt) and Pt/Beta (1 wt% Pt) estimated from the CO chemisorption measurements are given in Table 1. As observed, the metal dispersion on the WZr support decreases with increasing the metal loading from 0.6 to 1 wt%. Moreover, at the same Pt loading (1 wt%) the metal is better dispersed on the zeolite support.

The state of Pt in the calcined and reduced Pt-containing catalysts has also been studied by XPS. Table 2 lists the binding energies obtained for several electron levels of 1Pt/Beta and 1Pt/WZr catalysts, before and after *in situ* reduction in hydrogen at 723 and 523 K, respectively.

Binding energy of Pt4$f_{7/2}$ for calcined Pt/Beta zeolite was 72.1 eV, indicating the presence of Pt^{2+} on the surface. Nevertheless, the presence of platinum in a more oxidate state is not discarded due to the interference originated from the Al2*p* transition. The value of the surface (XPS) Pt concentration (0.4 wt%) differed substantitally from that of the bulk (1 wt%), suggesting a good dispersion of the metal in the microporous zeolite matrix, in agreement with the CO chemisorption measurements. After treatment in a reducing atmosphere at 723 K, the Pt4$f_{7/2}$ binding energy decreased by 1.7 eV, indicating the reduction of Pt^{2+} to metal, and the amount of surface platinum increased (0.6 wt%), indicating the migration of Pt particles from the bulk matrix to the zeolite surface during the reduction process. Although these values are unusually low with respect to the expected BE in clean metal surfaces, similar values have been reported for Pt^{2+} and Pt^0 species in different Pt-supported samples (33, 34).

Figure 3 illustrates the Pt4*f* spectra obtained for the sample 1Pt/WZr (1 wt% Pt) before and after reduction in hydrogen at 523 K. The calcined sample shows two peaks at ca. 73.6 and 74.9 eV ascribed to Pt^{2+} and Pt^{4+}, respectively (Table 2). After *in situ* reduction these peaks are shifted to lower binding energy. However, it was found that a substantial amount of the surface platinum in this catalyst remained as Pt^{2+}, as can be derived from the peak observed at 74.0 eV (Fig. 3b). The Pt^{2+}/Pt^0 ratio in the reduced sample was estimated to be ca. 0.7 from the integrated intensities of the corresponding signals. The low reducibility of the dispersed platinum particles present as Pt^{2+} on the WZr support could be interpreted by a strong interaction between Pt and the surface W^{6+} species. These results are almost qualitatively in agreement with the TPR data discussed above.

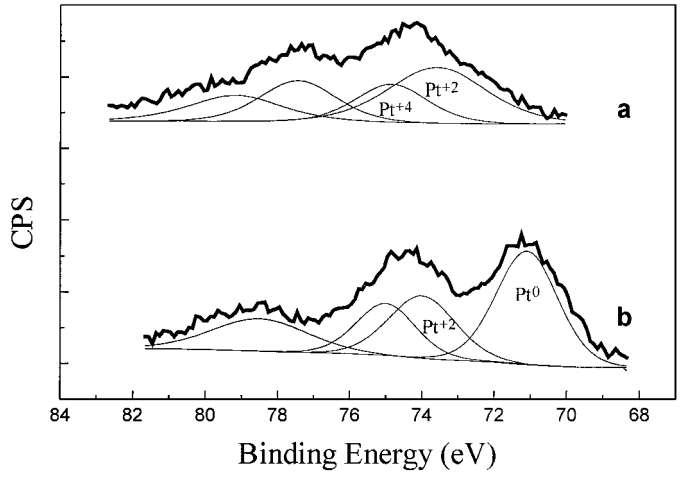

FIG. 3. XPS subband analysis of Pt4*f* region for (a) 1Pt/WZr calcined in dry air at 1073 K and (b) 1Pt/WZr reduced *in situ* in flowing H_2 at 523 K.

The W4f XPS spectra of this sample before and after treatment under reducing atmosphere are shown in Fig. 4. The W4$f_{7/2}$ transition for the calcined sample could be fitted with only one peak at 35.6 eV, attributed to W^{6+} (35). No peaks attributed to W^{4+} (ca. 34.0 eV B.E.) or W^0 (ca. 32.0 eV BE) were observed in the sample calcined at 1073 K, in

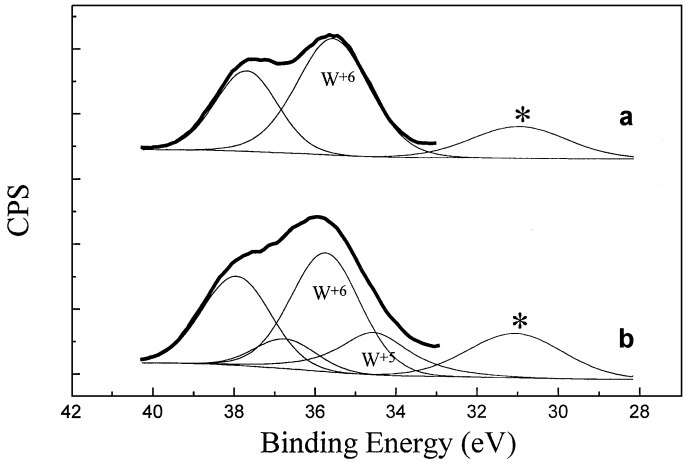

FIG. 4. XPS subband analysis of W4*f* region for (a) 1Pt/WZr calcined in dry air at 1073 K and (b) 1Pt/WZr reduced *in situ* in flowing H_2 at 523 K. Peaks with the symbol * indicate the Zr2*p* transition.

agreement with previous work (15). However, a qualitative change in the W4*f* transition is observed after reduction in hydrogen at 523 K, and a new peak at ca. 34.6 eV (W4$f_{7/2}$) appeared that we have tentatively assigned to W^{5+} species. The formation of these species could be favored by the Pt–W interaction on the catalyst surface. In fact, the TPR data indicated a higher reducibility of W^{6+} in the presence of Pt.

3.2. Simultaneous Hydroconversion of n-Heptane and Benzene

3.2.1. Influence of reduction temperature on the activity of Pt/WO_x–ZrO_2. Although it has been previously reported that the use of high reduction temperatures (typically above 623 K) causes a decrease of the isomerization activity of Pt/WO_x–ZrO_2 catalysts (26, 27), there are no studies concerning the effect of this parameter on their hydrogenation activity. Here we have studied the influence of the temperature of reduction on both the isomerization and hydrogenation activities of sample 0.6Pt/WZr during the conversion of the *n*-heptane/benzene mixture at 493 K in the absence of sulfur, and the results are presented in Table 3. It is seen that both the *n*-heptane and the benzene conversions decrease when increasing the reduction temperature from 523 to 723 K. However, it appears that this parameter has a larger influence on the isomerization activity of the catalyst. In view of these results, all the catalytic data presented hereinafter for the Pt/WO_x–ZrO_2 catalysts were obtained using a reduction temperature of 523 K.

3.2.2. Pt/WO_x–ZrO_2 versus Pt/Beta in the absence of sulfur. The conversion of a *n*-heptane/benzene feed mixture (25 wt% benzene) was first carried out in the absence of sulfur over the 0.6Pt/WZr and 1Pt/Beta catalysts presenting different textural and acidic characteristics. The conversion of *n*-C_7 as a function of reaction temperature is presented in Fig. 5. In the absence of sulfur, benzene was totally converted over the two catalysts in the whole range of temperatures studied. As observed in Fig. 5, the temperature required to achieve a given *n*-C_7 conversion level was about

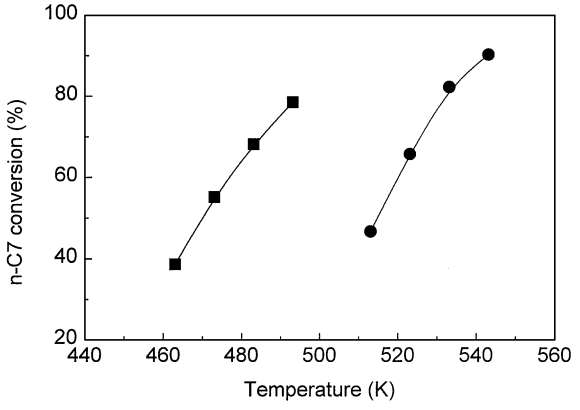

FIG. 5. *n*-Heptane conversion as a function of reaction temperature for the 0.6Pt/WZr (■) and 1Pt/Beta (●) catalysts. Reaction conditions: $P = 3.0$ MPa; WHSV $= 3.1$ h^{-1}, H_2/HC $= 10$.

40–45 K lower for the 0.6Pt/WZr sample than for 1Pt/Beta, suggesting that the former catalyst contains acid sites of a higher strength, in agreement with the NH_3-TPD data. Similarly, Santiesteban *et al.* (25) reported a higher activity for *n*-pentane isomerization over a tungsten–zirconia catalyst as compared to zeolite Beta. The isomerization and hydrogenation activities of the two catalysts, expressed as TOF (mol of *n*-heptane or benzene converted per min and exposed surface Pt), are given in Table 4.

As shown in Fig. 6, both catalysts presented a high selectivity for isomerization, but the 0.6Pt/WZr sample was slightly more selective to *iso*-C_7 for *n*-C_7 conversions above 60%. Thus, at ca. 75% conversion the selectivity to isoheptanes was ca. 90% and ca. 87% for 0.6Pt/WZr and 1Pt/Beta, respectively. However, the distribution of the *iso*-C_7 compounds differed considerably for the two catalyst, as observed in Table 5, when compared at a similar *iso*-C_7 yield

TABLE 3

Influence of Reduction Temperature on the Isomerization and Hydrogenation Activities of Pt/WO_x–ZrO_2 Catalyst (0.6 wt% Pt)

	Conversion (%)	
T_{red} (K)	*n*-Heptane	Benzene
523	78.3	100.0
623	54.0	96.9
723	29.2	84.5

Note. Reaction conditions: $T = 493$ K, $P = 3.0$ MPa, H_2/HC $= 10$, WHSV $= 3.1$ h^{-1}).

TABLE 4

Activity of 0.6Pt/WZr and 1Pt/Beta Catalysts, Expressed as TOF, for the Hydroisomerization and Hydrogenation Reactions at Different Reaction Temperatures

		TOF (mol min^{-1} at-gr_{Pt}^{-1})[a]	
Catalyst	T (K)	Hydroisomerization	Hydrogenation
0.6Pt/WZr	463	10.2	11.3
	473	14.6	11.3
	483	18.0	11.3
	493	20.8	11.3
1Pt/Beta	513	8.3	7.7
	523	11.7	7.7
	533	14.7	7.7
	543	16.1	7.7

[a] Calculated as mol of reactant (*n*-heptane or benzene) converted per min and at-gr of exposed Pt according to the metal dispersion obtained from CO chemisorption (Table 1).

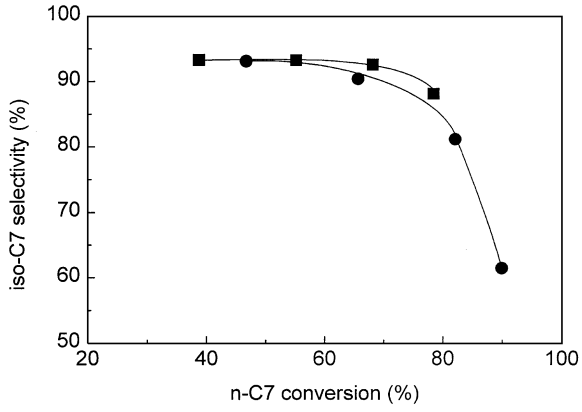

FIG. 6. Selectivity to *iso*-heptanes against the *n*-C_7 conversion for the 0.6%Pt/WZr (■) and 1%Pt/Beta (●) catalysts. Reaction conditions as in Fig. 5.

(ca. 50 wt%). For both catalysts the monobranched 2-MH and 3-MH were the predominent products, the two isomers being formed in almost equimolar amounts. However, owing to the lower reaction temperature, $Pt/WO_x–ZrO_2$ produced a slightly higher proportion of multibranched isomers. Among the dibranched products, 2,2-DMP, 2,3-DMP, and 2,4-DMP were the predominant isomers for both catalysts, while 3,3-DMP occurred in a lower concentration. Cycloalkanes were formed in small amounts on the two catalysts.

The distribution of the hydrocracking C_1–C_6 products, excluding CH and MCP, is presented in Table 6. It is readily noted the relatively large amounts of C_6 compounds produced over the two catalysts, which are formed by the acid-catalyzed ring opening of the MCP and CH cycloalkanes. The larger concentration of C_6 products obtained with 0.6Pt/WZr indicates a higher activity for C–C cleavage in the naphthenic rings over this catalyst as compared to 1Pt/Beta. As expected, C_3 and C_4 were the major products formed by hydrocracking of *n*-heptane. However, the concentration of $C_3 + C_4$ (even excluding the C_6 products) is larger on 1Pt/Beta than on 0.6Pt/WZr, suggesting that there is a higher contribution of the classic bifunctional hydrocracking mechanism (36, 37) for the former catalyst. According to the ideal bifunctional mechanism, hydrocracking of *n*-C_7 would result in equimolar amounts of C_3 and C_4. Indeed, the C_4/C_3 molar ratio was very close to unity for both catalysts, as observed in Table 6. In order to explain the detailed product distribution obtained during the conversion of *n*-C_7 on Pd/Beta catalysts, Blomsma *et al.* (11, 12) have proposed that there is a certain contribution of a dimerization-cracking (DC) mechanism, besides the classic hydrocracking, the extent of which depends on the Pd content of the catalyst. Such a DC mechanism makes it possible to explain the excess of C_4 as compared to C_3, as well as the formation of C_5 and C_6 products from the hydrocracking of *n*-heptane. The results presented in Table 6 suggest that, under our reaction conditions, the DC mechanism has only a minor contribution to the hydrocracking performance of the two Pt-catalysts studied. On the other hand, the relative concentration of C_1 and C_2 products was low for the two catalysts, although their concentration in the hydrocracking products was higher for 0.6Pt/WZr. This indicates that the hydrogenolysis activity of Pt is higher when supported on the tungsten–zirconia material than on the zeolite, even considering that the two catalysts compared here presented a similar Pt dispersion (Table 1).

TABLE 5

Distribution of *iso*-C_7 Products over the $Pt/WO_x–ZrO_2$ (0.6%Pt) and Pt/Beta (1%Pt) Catalysts

Sample	0.6Pt/WZr	1Pt/Beta
Temperature (K)	493	533
iso-C_7 yield (wt%)	51.7	49.9
Distribution of *iso*-C_7 (%)		
2,2,3-TMB	1.10	0.73
2,2-DMP	8.18	6.27
2,4-DMP	8.06	7.58
3,3-DMP	3.69	3.33
2,3-DMP	9.63	9.35
DMCPs[a]	0.18	0.24
Total di + tribranched	*30.84*	*27.50*
2-MH	32.97	34.12
3-MH	33.44	35.29
3-EP	2.44	2.63
MCH	0.29	0.42
ECP	0.02	0.04
Total monobranched	*69.16*	*72.50*

[a] 1,1- + 1,2- + 1,3-Dimethylcyclopentane.

TABLE 6

Distribution of Hydrocracking Products over the $Pt/WO_x–ZrO_2$ (0.6%Pt) and Pt/Beta (1%Pt) Catalysts

Sample	0.6Pt/WZr	1Pt/Beta
Temperature (K)	493	533
C_1–C_6 yield[a] (wt%)	7.0	10.8
Distribution (mol%)		
C_1	1.16	0.20
C_2	0.84	0.23
C_3	41.21	46.29
iso-C_4	39.84	46.08
n-C_4	2.96	1.11
iso-C_5	0.97	0.36
n-C_5	0.70	0.23
iso-C_6	8.05	3.23
n-C_6	4.27	2.27
$C_1 + C_2$	2.00	0.43
$C_3 + C_4$	84.01	93.48
C_4/C_3 molar ratio	1.04	1.02
iso-C_4/*n*-C_4	13.5	41.5

[a] Excluding benzene, CH, and MCP.

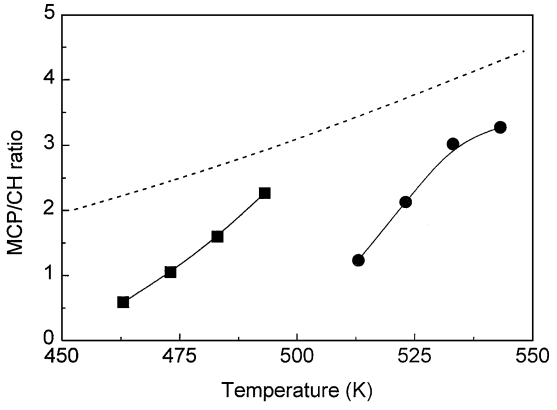

FIG. 7. Variation of the methylcyclopentane/cyclohexane (MCP/CH) ratio with reaction temperature for the (■) 0.6Pt/WZr and (●) 1Pt/Beta catalysts. The equilibrium ratio is given by the dashed line.

As said before, the conversion of benzene was 100% for the two catalysts in the whole range of temperatures studied. The main products obtained from the hydrogenation of benzene were cyclohexane (CH) and its higher octane methylcyclopentane (MCP) isomer, with a total selectivity to CH + MCP above 90% even at the highest temperatures applied. As predicted by the thermodynamic equilibrium, the concentration of MCP increased with reaction temperature for the two catalysts (Fig. 7). However, for a given *n*-C_7 conversion, the MCP/CH ratio was higher for 1Pt/Beta than for 0.6Pt/WZr owing to the higher temperatures used for the former catalyst.

3.2.3. Sulfur resistance of Pt-supported catalysts. The stability of the catalysts toward sulfur poisoning was studied by adding 200 ppm of S as 2-methylthiophene (2MT) to the *n*-heptane/benzene feed mixture. The relative change of catalyst activity for *n*-C_7 hydroconversion and benzene hydrogenation with time on stream (TOS) is presented in Fig. 8 for the 0.6Pt/WZr, 1Pt/WZr, and 1Pt/Beta catalysts. For all three catalysts the *n*-C_7 conversion starts to decline after a few min from the addition of sulfur and then tends to stabilize at larger TOS. No significant differences in the deactivation rate were observed for the Pt/WZr samples containing different Pt concentration. It is readily seen in Fig. 8a that the relative activity for *n*-C_7 hydroconversion in much higher for Pt/Beta than for Pt/WZr (irrespective of Pt content), indicating that the former catalyst is more sulfur resistant under the reaction conditions used. Thus, the zeolite-based catalyst retained a high activity in the presence of S (about 75% of the initial *n*-C_7 conversion is obtained after ca. 400 min on stream), while the Pt/WZr catalysts loosed ca. 80% of their initial activity for converting *n*-C_7 after ca. 300 min on stream.

The superior sulfur resistance of the Pt/zeolite catalyst is clearly manifested when comparing the relative hydrogenation activities of the two types of catalysts (Fig. 8b). Thus, the conversion of benzene was kept at the same initial value (100% conversion) over 1Pt/Beta in the whole range of TOS studied, $(Xbz)_t/(Xbz)_0 = 1$, whereas it decreased from 100% to ca. 4% for 1Pt/WZr and to 0% for 0.6Pt/WZr after about 300 min on stream. Taking into account the rate of S addition (9.75×10^{-7} at-g S/min) and the amount of exposed surface Pt (6.52×10^{-5} at-g Pt in 3 g of catalyst), as derived from CO chemisorption experiments, it is easily deduced that the Pt/Beta catalyst maintains intact its hydrogenation ability even for a S/Pt atomic ratio of ca. 6 (TOS = 407 min). The different hydrogenation activity of the two catalysts in the presence of sulfur might suggest a different deactivation mechanism of the hydrogenation sites in both catalytic systems. Nevertheless, and even assuming that the operating deactivation mechanism is similar for the two type of catalysts, the higher sulfur resistance of the Pt/Beta as compared to Pt/WZr could be explained considering the following factors: (a) the higher amount of exposed Pt atoms in Pt/Beta, (b) the strong interaction of part of the surface Pt atoms in Pt/WZr with the support, as evidenced by TPR and XPS, which further reduces the amount of Pt^0 species on the catalyst surface, and (c) the possibility of formation of sulfur-tolerant electron-deficient Pt particles in

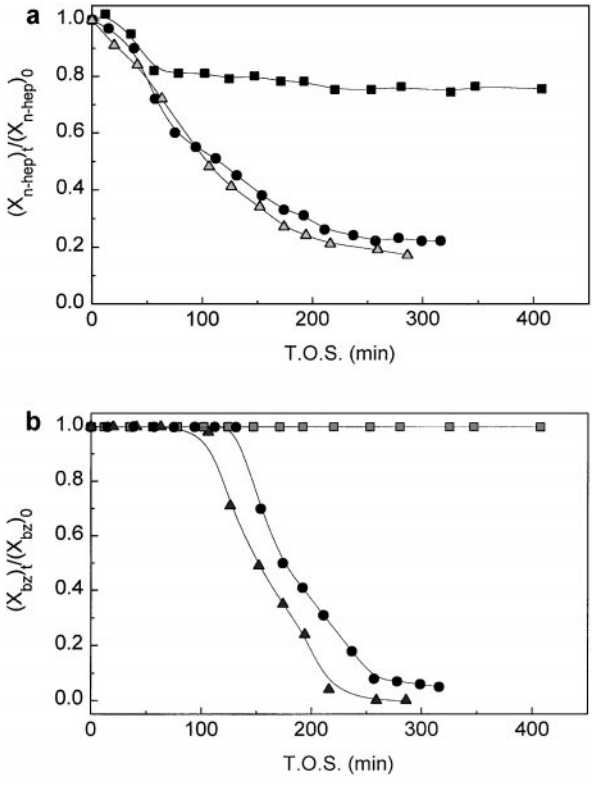

FIG. 8. Relative change of catalyst activity for *n*-C_7 hydroconversion (a) and benzene hydrogenation (b) with TOS during the conversion of a *n*-C_7/benzene feed containing 200 ppm sulfur: (■) 1Pt/Beta, (▲) 0.6Pt/WZr, (●) 1Pt/WZr. Reaction conditions: $T = 493$ K for Pt/WZr and 533 K for 1Pt/Beta, $P = 3.0$ MPa, WHSV = 3.1 h^{-1}, H_2/HC = 10.

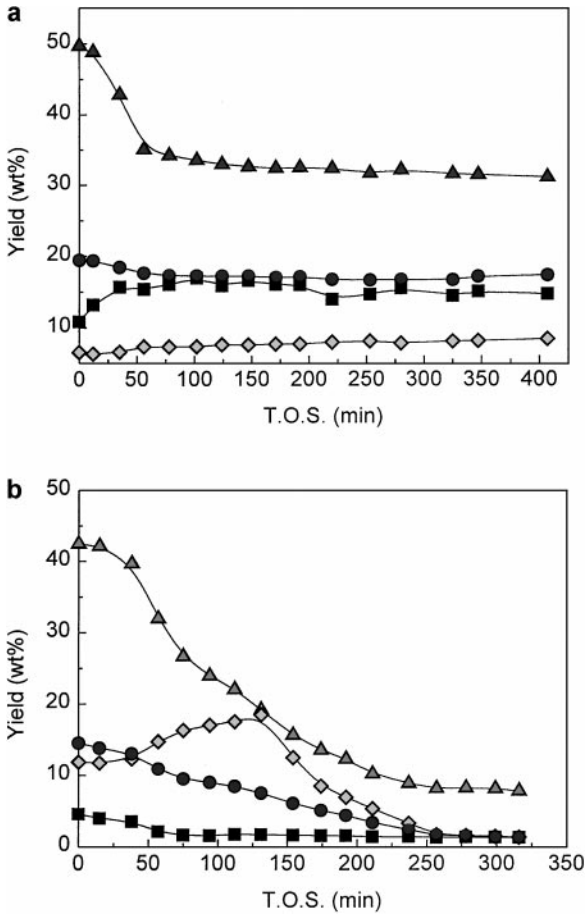

FIG. 9. Change of product product yields with TOS for (a) 1Pt/Beta and (b) 1Pt/WZr catalysts during the conversion of *n*-C_7/benzene in the presence of 200 ppm sulfur: (■) C_1–C_6, (▲) *iso*-C_7, (◆) cyclohexane, (●) methylcyclopentane. Reaction conditions as in Fig. 8.

the zeolite cavities by interaction with the zeolitic protons (18–23).

Figure 9 shows the influence of sulfur poisoning on the different product yields for the Pt/WZr and Pt/Beta catalysts containing 1 wt% Pt. For Pt/Beta (Fig. 9a) the yield to *iso*-heptanes initially decreased during the first 60–70 min TOS and then reached a nearly steady value of about 62% of the initial yield (TOS = 0). In the case of Pt/WZr (Fig. 9b), the *iso*-C_7 yield continuously decreased with time, reaching a value of ca. 20% of the initial yield after ca. 300 min on stream. For both catalysts the loss of *iso*-C_7 was accompanied by a decrease of isomerization selectivity in favor of cracking products (C_1–C_6), indicating that the nearly ideal bifunctional isomerization mechanism observed in the absence of sulfur was no longer operative in the presence of sulfur.

Figure 9b also shows that, for Pt/WZr, the CH yield increased during the first 125 min TOS, that is during the period for which benzene was totally hydrogenated (Fig. 8b), and then decreased when benzene conversion fell down below 100%. By contrast, the MCP yield, formed by isomerization of CH on the acid sites, monotonically decreased during the run. Also in the case of Pt/Beta catalyst, which gives 100% benzene conversion along the run, the CH yield slightly increased in detriment of MCP.

The decrease of *iso*-C_7 yield and MCP/CH ratio observed from the initial reaction stages, when the hydrogenation of benzene is 100% over the two catalysts, can be explained considering the poisoning, by coke deposits, of those acid sites which are close to the Pt atoms that are being deactivated by sulfur and thus having a much lower dehydrogenation–hydrogenation activity. The results obtained indicate that poisoning of acid sites occurs faster for the Pt/WZr catalyst as compared to Pt/Beta, owing to a rapid loss of the hydrogenation capacity of the former catalyst which limits the desorption of the olefinic intermediates formed during the isomerization reactions.

3.2.4. Reversibility/irreversibility of the deactivation process. The reversibility/irreversibility of the deactivation process was also studied by feeding again the sulfur-free *n*-C_7/benzene mixture after the period of deactivation with the sulfur containing feed. The steady-state relative isomerization and hydrogenation activities observed for the 1Pt/Beta and 1Pt/WZr catalysts during the transient kinetic experiments are shown in Table 7. The activity for *n*-C_7 isomerization of 1Pt/Beta was almost restored and reached 93% of its initial isomerization activity in about 1.5 h. Although the hydrogenation activity was kept to 100%, an increase of the MCP/CH ratio from 2.07 to 2.86 was noticed in the same period of time, approaching the value of 2.99 obtained for this catalyst before the sulfur deactivation experiment (Table 7). A different behavior was observed for the 1Pt/WZr catalyst. In this case the hydrogenation activity was practically fully restored, reaching a steady value of ca. 95% benzene conversion after about 9 h of restarting the sulfur-free mixture. However, the MCP/CH ratio did

TABLE 7

Relative Isomerization and Hydrogenation Activities and MCP/CH Ratio Obtained during the Conversion of *n*-C_7/Benzene over 1Pt/Beta and 1Pt/WZr Catalysts in the Transient Kinetic Experiments

Catalyst	Experiment[a]	Relative activity		MCP/CH ratio
		n-C_7 isomerization	Benzene hydrogenation	
1Pt/Beta	A	1	1	2.99
	A + B	0.75	1	2.07
	A + B + A	0.93	1	2.86
1Pt/WZr	A	1	1	1.22
	A + B	0.21	0.05	0.96
	A + B + A	0.26	0.95	0.47

[a] A, sulfur-free feed; B, 200 ppm sulfur feed.

not further increase but decreased with respect to the value obtained in the presence of 200 ppm sulfur (Table 7). On the other hand, the relative activity of 1Pt/WZr for *n*-C_7 isomerization experienced a slight increase from ca. 21% (after sulfur deactivation) to ca. 26% even after 12 h of restarting the sulfur-free feed. These transient kinetic experiments showed that deactivation of the hydrogenation sites (Pt) by sulfur is a reversible process for both types of catalysts. They also showed that the partial loss of isomerization activity observed during the sulfur deactivation experiments is almost reversible for Pt/Beta, while it is irreversible for Pt/WO_x–ZrO_2. These results could be explained considering that poisoning of the acid sites, responsible for *n*-C_7 and cyclohexane isomerization, in the latter catalyst by coke deposits extensively occurred in the presence of sulfur owing to the practically total deactivation of the hydrogenation sites. On the contrary, the high hydrogenation activity of the Pt/Beta catalyst maintained with the sulfur containing feed prevented the extensive coking of the zeolite acid sites. Further experiments to determine the amount and nature of the coke deposits formed on both catalysts in the absence and presence of sulfur in the feed mixture are in progress.

4. CONCLUSIONS

Pt/Beta and Pt/WO_x–ZrO_2 were found to be suitable catalysts for carrying out the simultaneous hydroisomerization of *n*-heptane and hydrogenation of benzene (25 wt% in *n*-C_7) in the presence of hydrogen. Thus, in the absence of sulfur, both catalysts displayed high selectivity to *iso*-heptanes (ca. 90% at ca. 75% *n*-C_7 conversion), with benzene being totally converted with a selectivity to CH + MCP above 90% in the whole range of temperatures studied. Owing to the higher strength of the acid sites of the WO_x–ZrO_2 as compared to the Beta zeolite, the temperature required to achieve a given *n*-C_7 conversion was about 40–45 K lower for the former catalyst. Consequently, the concentration of the high-octane dimethylpentanes (DMP) and trimethylbutanes (TMB) in the *iso*-C_7 fraction was larger for the Pt/WO_x–ZrO_2 catalyst. However, as the isomerization of CH into its higher octane MCP isomer is thermodynamically favored at higher temperatures, the MCP/CH ratio was higher for the Pt/Beta sample. When 200 ppm sulfur is added to the *n*-heptane/benzene feed mixture, a decrease of the catalyst activity during the initial reaction stages was observed for the two catalysts, but Pt/Beta was found to be much more sulfur resistant than Pt/WO_x–ZrO_2. Thus, in the presence of sulfur the Pt/Beta catalyst retained about 60% of its initial isomerization activity, while the residual isomerization activity was only about 20% for Pt/WO_x–ZrO_2. Moreover, the presence of sulfur did not affect the hydrogenation activity of Pt/Beta in the reaction times studied, but strongly inhibited the hydrogenation capacity of Pt/WO_x–ZrO_2. Although a different deactivation mechanism of the hydrogenation sites for the two catalysts cannot be discarded, the fact that almost all the surface Pt atoms in the reduced Pt/Beta catalyst were in the metallic state, Pt^0, whereas about 40% of the surface Pt in the reduced 1Pt/WZr catalyst (as observed by XPS) existed as Pt^{2+}, might also explain the faster poisoning of the hydrogenation sites in Pt/WZr as compared to Pt/Beta. Moreover, the possibility of formation of electron-deficient Pt particles in the zeolite cavities by interaction of the Pt with the zeolitic protons, might also account for the higher sulfur resistance of the Pt/Beta catalyst. Deactivation of the hydrogenation sites in the presence of sulfur was seen to be a reversible process for the two catalysts. However, the low hydrogenation activity of Pt/WZr observed with the sulfur containing feed produced the irreversible deactivation of the acid sites by coke deposits and, consequently, of the isomerization activity of the catalyst. On the contrary, the isomerization activity of Pt/Beta was almost restored after feeding again the sulfur-free mixture. In this case, the high hydrogenation activity shown by this catalyst during the sulfur deactivation experiment prevented the extensive formation of coke on the zeolite acid sites.

ACKNOWLEDGMENTS

Financial support by the Comisión Interministerial de Ciencia y Tecnología (CICYT) of Spain is gratefully acknowledged (Project MAT97-1010). M. A. Arribas thanks the Generalitat Valenciana for a postgraduate scholarship. The authors thank Dr. F. Rey for the CO chemisorption measurements.

REFERENCES

1. Bour, G., Schwoerer, C. P., and Asselin, G. F., *Oil Gas J.* **68**, 43 (1970).
2. Ware, K. J., and Richardson, A. H., *Hydroc. Process.* **51**, 11 (1972).
3. Hancsók, J., and Holló, A., *Pet. Coal* **39**, 4 (1997).
4. Chen, J.-K., Martin, A. M., and John, V. T., *J. Catal.* **111**, 425 (1988).
5. Martin, A. M., Chen, J. K., and John, V. T., *Prepr. Am. Chem. Soc. Div. Pet. Chem.*, New York City Meeting, August 25–30, 1991.
6. Minachev, K. M., Kharlamov, V. V., Shkitov, A. M., and Fomin, A. S., *Mendeleev Commun.* 166 (1993).
7. Chao, K., Wu, H., and Leu, L., *Appl. Catal. A* **143**, 223 (1996).
8. Guisnet, M., and Fouche, V., *Appl. Catal.* **71**, 307 (1991).
9. Wang, Z., Kamo, A., Yoneda, T., Komatsu, T., and Yashima, T., *Appl. Catal. A* **159**, 119 (1997).
10. Del Gallo, P., Pham-Huu, C., York, A. P. E., and Ledoux, M. J., *Ind. Eng. Chem. Res.* **35**, 3302 (1996).
11. Blomsma, E., Martens, J. A., and Jacobs, P. A., *J. Catal.* **155**, 141 (1995).
12. Blomsma, E., Martens, J. A., and Jacobs, P. A., *J. Catal.* **159**, 323 (1996).
13. Iglesia, E., Barton, D. G., Soled, S. L., Miseo, S., Baumgartner, J. E., Gates, W. E., Fuentes, G. A., and Meitzner, G. D., *Stud. Surf. Sci. and Catal.* **101**, 533 (1996).
14. Comelli, R. A., Canavese, S. A., and Figoli, N. S., *Catal. Lett.* **55**, 177 (1998).
15. Vaudagna, S. R., Canavese, S. A., Comelli, R. A., and Figoli, N. S., *Appl. Catal. A* **168**, 93 (1998).
16. Vaudagna, S. R., Comelli, R. A., and Figoli, N. S., *Appl. Catal. A* **164**, 265 (1997).

17. Huang, Y. Y., Zhao, B. Y., and Xie, Y. C., *Appl. Catal. A* **171**, 75 (1998).
18. Jao, R.-M., Leu, L.-J., and Chang, J.-R., *Appl. Catal. A* **135**, 301 (1996).
19. Lee, J.-K., and Rhee, H.-K., *J. Catal.* **177**, 208 (1998).
20. Corma, A., Martínez, A., and Martínez-Soria, V., *J. Catal.* **169**, 480 (1997).
21. Song, Ch., and Schmitz, A. D., *Energy and Fuels* **11**, 656 (1997).
22. Yasuda, H., and Yoshimura, Y., *Catal. Lett.* **46**, 43 (1997).
23. Yasuda, H., Sato, T., and Yoshimura, Y., *Catal. Today* **50**, 63 (1999).
24. Hino, M., and Arata, K., *J. Chem. Soc., Chem. Commun.* 1259 (1987).
25. Santiesteban, J. G., Vartuli, J. C., Han, S., Bastian, R. D., and Chang, C. D., *J. Catal.* **168**, 431 (1997).
26. Iglesia, E., Barton, D. G., Soled, S. L., Miseo, S., Baumgartner, J. E., and Gates, W. E., "14th North American Catalysis Society Meeting, Extended Abstracts, Snowbird, 1995."
27. Larsen, G., and Petkovic, L. M., *Appl. Catal. A* **148**, 155 (1996).
28. Poster, D. L., *J. Am. Ceram. Soc.* **62**, 298 (1979).
29. Scofield, J. H., *J. Electron. Spectrosc. Relat. Phenom.* **8**, 129 (1976).
30. Vulli, M., and Starke, K., *J. Phys. E* **10**, 158 (1978).
31. Ji, W., Hu, J., and Chen, Y., *Catal. Lett.* **53**, 15 (1998).
32. Larsen, G., Lotero, E., and Parra, R. D., *Stud. Surf. Sci. Catal.* **101**, 543 (1996).
33. Hino, M., and Arata, K., *Appl. Catal. A* **169**, 151 (1998).
34. Arai, M., Takada, Y., Ebina, T., and Shirai, M., *Appl. Catal. A* **183**, 365 (1999).
35. Briggs, D., and Seah, M. (Eds.), "Practical Surface Analysis." Wiley, New York, 1994.
36. Weitkamp, J., Jacobs, P. A., and Martens, J. A., *Appl. Catal.* **8**, 123 (1983).
37. Martens, J. A., Jacobs, P. A., and Weitkamp, J., *Appl. Catal.* **20**, 239 (1986).